Special Issue: The Impact of Upper Pleistocene Climatic and Environmental Change on Hominin Occupations and Landscape Use, Part 1

The Sunny Side of the Ice Age: Solar Insolation as a Potential Long-Term Pacemaker for Demographic Developments in Europe Between 43 and 15 ka Ago

ANDREAS MAIER
Institute of Prehistoric Archaeology, University of Cologne, Bernhard-Feilchenfeld-Str. 11, 50969 Cologne, GERMANY; a.maier@uni-koeln.de

PATRICK LUDWIG
Institute of Meterology and Climate Research; Department Troposphere Research; Regional Climate and Weather Hazards; Karlsruhe Institute of Technology, Wolfgang-Gaede-Str. 1, 76131 Karlsruhe, GERMANY; patrick.ludwig@kit.edu

ANDREAS ZIMMERMANN
Institute of Prehistoric Archaeology, Collaborative Research Centre 806, University of Cologne, Bernhard-Feilchenfeld-Str. 11, 50969 Cologne, GERMANY; a.zimmermann@uni-koeln.de

ISABELL SCHMIDT
Institute of Prehistoric Archaeology, Collaborative Research Centre 806, University of Cologne, Bernhard-Feilchenfeld-Str. 11, 50969 Cologne, GERMANY; isabell.schmidt@uni-koeln.de

submitted: 30 June 2019; accepted: 25 August 2020

ABSTRACT

After a decade of research under the auspices of the project 'Population dynamics: Land use patterns of populations between the Upper Pleistocene and Middle Holocene in Europe and the Middle East,' a consistent sequence of high-resolution paleodemographic datasets has been compiled, spanning the entire Upper Paleolithic from roughly 43 to 15 ka. When viewed in a diachronic perspective, long-term trends of increasing and decreasing population sizes and densities, as well as expanding and contracting areas of settlement activities (Core Areas), become evident. An environmental parameter with potentially strong impact on hunter-gatherer societies is solar insolation. The sun's energy available at any given time and place is one of the main factors influencing plant growth. The amount of plant biomass, in turn, largely determines the amount of animal biomass in a landscape. The latter was the most important source of energy for European Upper Paleolithic hunter-gatherers. Here, we aim to assess the potential influence of changes in solar insolation on paleodemographic development in Western and Central Europe between 43 and 15 ka. To this end, we present estimates on the number, density, and spatial distribution of hunter-gatherers for five consecutive Upper Paleolithic periods in Europe. Based on regional climate model data for the Last Glacial Maximum and solar insolation data, we calculate: 1) differences in the amount of Megajoule per square meter (MJm^{-2}), 2) start, end, and length of the growing season, as well as 3) summed temperatures during the entire duration and during the first 30 days of the growing season. A comparison shows that a moderate, steady increase of population size and an extension of the Core Areas between 43 and 29 ka coincides with an increase in the summed temperature, particularly during the first 30 days of the growing season. The period between 29 and 25 ka shows a pronounced population decline, a strong contraction of Core Areas and a withdrawal from higher latitudes. This coincides with a markedly delayed growing season, a decrease in summed temperatures, and a marked reduction in solar insolation during the early part of the growing season. Between 25 and 20 ka, we see consolidation and renewed growth in both numbers and densities of people and an expansion and merging of Core Areas in Western Europe. There is a slight gain in the energy available during the first half of the year. The growing season starts earlier and is of increasingly longer duration, coupled with rising summed temperatures. Between 20 and 15 ka, the meta-population grows strongly, Core Areas expand, and the higher latitudes become repopulated. This coincides with further-increasing summed temperatures and an ever-earlier start to the growing season. Additionally, the gain in available solar energy during the early phase of the growing season is particularly pronounced. These findings indicate that solar insolation and its effects on an

ecosystem's phenological configuration over different trophic levels is indeed an important factor in the long-term demographic development of Paleolithic hunter-gatherers.

This special issue is guest-edited by William Davies (Centre for the Archaeology of Human Origins, University of Southampton) and Philip R. Nigst (Department of Prehistoric and Historical Archaeology, University of Vienna).

INTRODUCTION

Over the last two decades, several innovative approaches to paleodemography (Bocquet-Appel and Demars 2000; Bocquet-Appel et al. 2005; French 2015; French and Collins 2015; Kretschmer 2015; Maier et al. 2016; Maier and Zimmermann 2017; Schmidt and Zimmermann 2019; Tallavaara et al. 2015) and population genetics (e.g., Fu et al. 2016; Posth et al. 2016) have advanced research on Upper Paleolithic population dynamics. At the same time, a number of factors have been discussed with regard to their explanatory potential for the observed demographic developments; these include technological gain and loss, social organization and norms, and environment (Boserup 1965; Bradtmöller et al. 2010; French 2018; Gamble 1999; Gamble et al 2004; Henderson and Loreau 2019; Roebroeks 2006). To be clear, social and technological factors certainly play an important role in human population dynamics, and innovations or a loss of technological knowledge can affect population dynamics strongly. However, for large-scale studies such as this one, there are two major problems for exploring their impact on the number, density, and distribution of humans in a landscape. The first problem is that social, technological, and demographic developments are interdependent, where social organization may influence demographic developments and vice versa. Thus, it is extremely difficult to distinguish cause from effect. The second problem is that social organization and technological repertoires depend on human decision making, which is observable at a different timescale than long-term developments. Long-term demographic developments over a period of several millennia are incompatible with human decision-making. Environmental change, on the other hand, can be meaningfully observed at small and large temporal scales. The impact of human societies on the environment during the Paleolithic is subject to debate. Topics range from reflections on negative impacts on forest cover (Kaplan et al. 2016) to the involvement in the extinction of megafauna (e.g., Koch and Barnosky 2006; Sandom et al. 2014). However, during the entire period of observation between 43 and 15 kiloannum (ka), human influence on environment and particularly on climate seems to have been comparatively small, making it relatively easy to distinguish between cause and effect. Nonetheless, proving a causal relationship remains difficult, not least because of incompatible or insufficient temporal and spatial resolution in the archaeological data. The introduction of absolute numbers and densities of human populations as a new, quantified variable at a comparatively high spatial and temporal resolution is a first step in addressing this problem. While acknowledging the importance of social and technological factors for demographic developments, this paper will focus on environmental change and its explanatory potential for the changes we observe in the currently available paleodemographic data.

The data for successive time-slices (Kretschmer 2015; Maier et al. 2016; Maier and Zimmermann 2017; Schmidt and Zimmermann 2019) have a temporal resolution of between 4 and 5 ka. Temperature change, as captured in the ice-core records, varies at a frequency much too high to be meaningfully compared to our data (Figure 1). Moreover, low temperatures alone are not a limiting factor for human settlement activities. On the contrary, it has been shown that some Paleolithic hunter-gatherer communities preferred permafrost over equally accessible non-permafrost areas (Demidenko 2018; Maier et al. 2016). However, it would be overstated to assume that environmental thresholds were virtually meaningless for well-adapted Paleolithic hunter-gatherers. Rather than temperature alone, the availability of animal biomass was probably a key factor to allow permanent settlement in a region (Kelly 1983; Mandryk 1993). The amount and diversity of animal biomass, in turn, is dependent on the amount and quality of primary plant biomass (Olff et al. 2002). A very important factor for the production of plant biomass is solar insolation (Monteith 1994). At the same time, this environmental parameter changes gradually and slowly, making it compatible with our demographic estimates (see Figure 1). Solar insolation affects plant biomass production in two primary ways. First, it drives air temperatures near the surface, one of the main factors determining the length of the growing season (Jiang et al. 2018). This correlation is so strong that temperature-based models to estimate insolation perform better than those based on sunshine, particularly when averaged to a monthly base (Hassan et al. 2016). Second, it provides the energy needed for photosynthesis, and there is a linear relationship between solar insolation and biomass production (Gosse et al. 1986). Therefore, it seems to be an important factor in an ecosystem's phenological configuration, i.e., in the timing of periodic life cycle parameters of plants and animals (Gienapp et al. 2014; Parmesan and Hanley 2015; Liu et al. 2016, Huang et al. 2019). Phenological shifts may be effective over different trophic levels and lead to mismatches in resource availability and predator-prey relations (Burrows et al. 2011; Ohlberger et al. 2014). It has

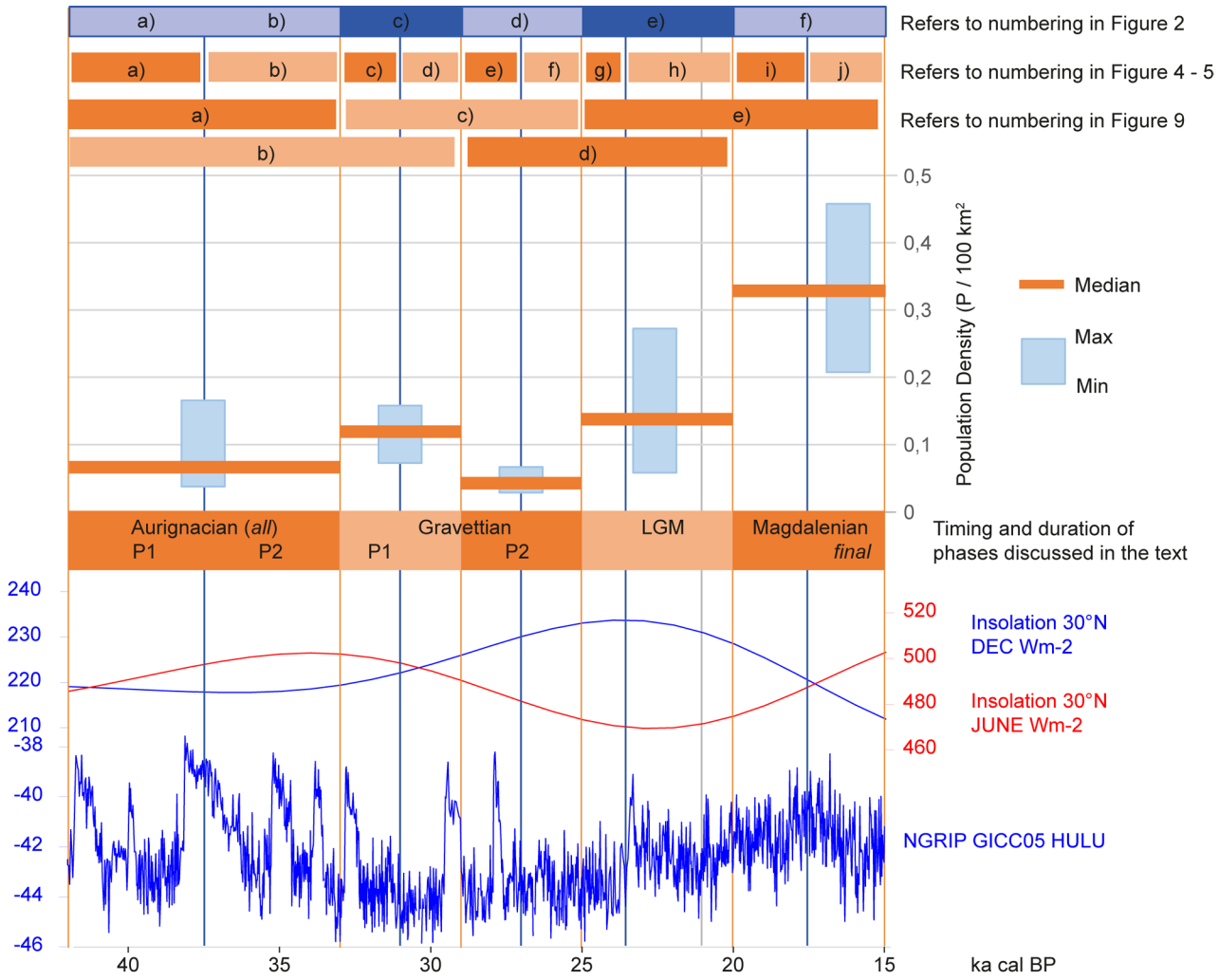

Figure 1. Overview on timeframe and temporal scales of data. Population density estimates are given for the generalized Total Area of Calculation (TAC) of 2.3 million km² (see Figure 2 for spatial extent), terminology for archaeological phases corresponds with Table 1. Note: estimates for the Magdalenian in total have not been calculated (see Kretschmer 2015), but would resemble those of the Final Magdalenian. Vertical lines indicate "insolation reference dates," blue lines indicate insolation values used for synchronic illustrations (Figure 2), orange lines for calculating differences in insolation for diachronic developments (see Figure 9), grey line at 21 ka indicates anchor point of the PMIP3 LGM climate model data. Timeframes covered in Figure 2 and 9 are indicated and labelled accordingly. Insolation (30° N, June and December) and GISP 2 Delta $^{18}O/^{16}O$ are taken from Climate Data CalPal (Weninger and Jöris 2008, accessed 27.06.2019).

been shown for birds that these mismatches affect migrating species particularly strongly when an expected food resource is not available upon arrival (Both et al. 2010; Mayor et al. 2017).

In the following sections, we will evaluate estimates of the number and density of people, as well as the position and extent of Core Areas, against insolation data for the period between 40 ka and 15 ka.

MATERIAL AND METHODS

PALEODEMOGRAPHIC AND SPATIAL DATA

The study used spatial information on site locations and raw material transport, as well as estimated demographic data for the periods of 42–33 ka (Aurignacian, Schmidt and Zimmermann 2019), 33–29 ka and 29–25 ka (Gravettian subdivided into an early phase 1 and later phase 2, Maier and Zimmermann 2017), 25–20 ka (LGM, Maier et al. 2016), and 20–14 ka (Magdalenian, Kretschmer 2015). The approach to estimate population sizes and densities, the "Cologne Protocol," was developed and described for Neolithic and younger periods (Zimmermann et al. 2009), and subsequently transferred and adapted to hunter-gatherer contexts (Kretschmer 2015). For details on the protocol, we refer the reader to Schmidt et al. (2021). Briefly, the protocol distinguishes areas of intensive use, so-called Core Areas, from areas which have been used ephemerally, occasionally (e.g. during short phases of perceived climatic amelioration), or even not at all. Core Areas thus provide the minimum, but also the most robust, evidence for human

TABLE 1. OVERVIEW OF TIMEFRAME AND DATABASE FOR EACH PHASE.

Archaeological Period	ka	Duration (ka)	Number of Sites Included	Number of Sites / ka	Core Areas (km²)	Population Size			Population Density Estimate per 2.3 M km²		
						min	median	max	min	median	max
Aurignacian (all)	42–33	9	382	43	**103,686**	**880**	**1,550**	**3,800**	0.038	0.067	0.165
Aur P1 (Proto/Early)	*n.a.*	*5*	*117*	*23*	***81,900***	*n.a.*	*n.a.*	*n.a.*	*n.a.*	*n.a.*	*n.a.*
Aur P2	*n.a.*	*4*	*317*	*79*	***128,600***	*n.a.*	*n.a.*	*n.a.*	*n.a.*	*n.a.*	*n.a.*
Gravettian P1	33–29	4	347	87	**243,039**	**1,660**	**2,760**	**3,610**	0.072	0.120	0.157
Gravettian P2	29–25	4	163	41	**123,810**	**660**	**1,000**	**1,530**	0.029	0.044	0.067
Last Glacial Maximum	25–20	5	396	79	**275,413**	**1,330**	**3,240**	**6,260**	0.058	0.141	0.272
Magdalenian (final)	20–15	5	1,002	200	**332,949**	**4,820**	**7,600**	**10,520**	0.210	0.330	0.458

presence on a large spatial *and* temporal scale (e.g., Klein et al. 2021). Core Areas were modelled within a defined map section, called Total Area of Calculation (TAC). The spatial distribution of Core Areas and the TAC used for the European Upper Paleolithic is given in Figure 2. In a next step, spatial information on lithic raw material transport was used to estimate the number of groups within a Core Area. Using information on group sizes from the ethnographic literature, the number and density of people within a Core Area and within the TAC were inferred. Table 1 reviews the basic data for the paleodemographic estimates. For the Magdalenian we used data from the final Magdalenian period only, instead of averaging the higher resolution data provided by Kretschmer (2015). Similarly, for reasons of comparability, the demographic density estimates presented in Table 1 were calculated based on a unified TAC, comprising 2,300,000km² and illustrated in Figure 2, thus partially differing from previously published estimates. Core Areas for the final Magdalenian located outside the TAC (e.g., in Great Britain and Italy) were not considered for calculating spatial differences in Core Area distributions.

ENVIRONMENTAL DATA

Insolation data, after Berger (1978), in Watts per square meter (Wm^{-2}) were obtained from the R package palinsol (Crucifix 2016) for twelve successive "insolation reference dates" at 42, 37.5, 33, 31, 29, 27, 25, 23.5, 21, 20, 17, and 15 ka (see Figure 1). These insolation reference dates were chosen to coincide with the boundaries and midpoints of the periods for the paleodemographic estimates, to provide an optimal fit of the data (see Figure 2). The only exception is the LGM period, for which two internal insolation reference dates are provided. This accounts for the observation of the transition between the Solutrean and Badegoulian in the archaeological record at around 23.5 ka, as well as for the anchor point of our climatic data at 21 ka, which is the focus time of the PMIP3 (Paleoclimate Modelling Intercomparison Project, Phase 3, Braconnot et al. 2012) LGM climate models. Averaged daily temperatures (2m above ground level) were obtained from a 30-year-long regional climate model simulation (horizontal grid spacing ~50km) with the WRF model (Weather Research and Forecasting, Skamarock et al. 2008) that was nested into the coarse gridded (~200km horizontal grid spacing) MPI-ESM-P (Max Planck Institute for Meteorology Earth System Model in Paleo model, Giorgetta et al. 2013) LGM simulation. The regional WRF model has been adapted to LGM boundary conditions (e.g., ice sheets, lowered sea level, orbital parameters), and is forced by 6-hourly MPI-ESM-P data at its lateral boundaries (Ludwig et al. 2017). Additionally, an adjustment of sea surface temperatures based on the MARGO project (Multiproxy Approach for the Reconstruction of the Glacial Ocean surface, MARGO Project Members 2009) yielded a better agreement of the WRF model results with the available proxy data (Ludwig et al. 2017). For comparison with the present-day, an additional WRF simulation was performed that was forced by MPI-ESM-P data for present day climate simulation.

In order to transform these data into information meaningful for the production of primary biomass, we estimated for each insolation reference date the available energy per month at a given latitude in Megajoules per square meter (MJm^{-2}), as well as the start, end, length, and summed temperature of the growing season.

To transfer monthly Wm^{-2} into monthly MJm^{-2}, we used the following function

$$MJm^{-2}_{month} = (Wm^{-2}/1000) \times ld_{lat} \times nd \times 3.6$$

where ld_{lat} is the length of daylight at a given latitude under current orbital conditions, nd is the number of days per month and 3.6 is the factor to transform kWh into MJ. Given the large scale of this study, we ignored insolation distortions introduced by local topography or daily differences due to cloud cover.

By most definitions, the growing season starts with six consecutive days of a mean daily temperature near the ground surface above 5°C, and ends with six consecutive days below 5°C of mean daily temperature (Jiang et al. 2018). Since mean daily temperatures in the model data were averaged over 30 years, increases and decreases are rather steady, and reversions are rare. In order to account for this increased steadiness, we calculated the length of the growing season as the number of days between the first of the first three consecutive days above 5°C and the last day before the first three consecutive days below 5°C.

In order to estimate the start, end, and length of the growing season at 50°N and 45°N for each of the twelve insolation reference dates, we used the finding by Van Meerbeeck et al. (2009: 44) that during Marine Isotope Stage (MIS) 3 an increase in 4 Wm^{-2} resulted in an increase of 1°C, based on the seasonal global mean July surface air temperature

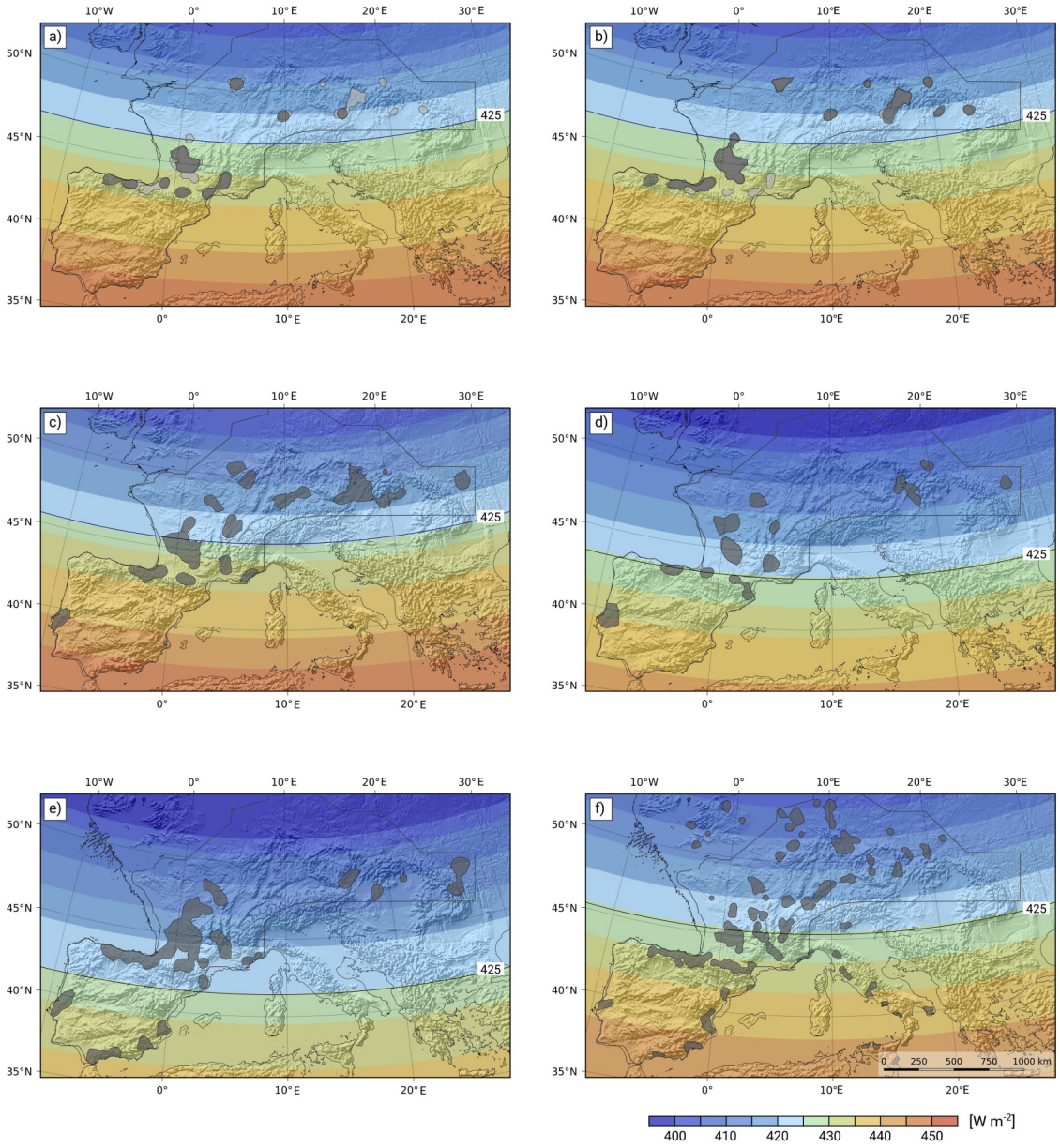

Figure 2. Distribution of Core Areas of the Upper Paleolithic plotted against insolation (Wm^{-2}) during growing season. For reasons of comparability, the growing season is set from April to September in this graph. Individual growing seasons are given in Figure 7 and Table 4. Latitudinal changes in insolation are highlighted by the 425 in Wm^{-2} isoline for visualization. Core Areas falling within the Total Area of Calculation (TAC, grey line) are considered during further analysis. a) and b): 42–33 ka (Aurignacian P1 (a) and P2 (b) plotted in dark grey onto Aurignacian all Core Areas in light grey), insolation at 37.5; c) 33–29 ka (Gravettian P1), insolation at 31 ka; d) 29–25 ka (Gravettian P2) insolation at 27 ka; e) 25–20 ka (LGM), insolation at 23.5 ka; f) 20–15 ka (Magdalenian final), insolation at 17 ka. Coastline is -75m below current sea-level (a and b), -80m b.c.s.l. (c and d), -120m b.c.s.l. (e) and -115m b.c.s.l. (f) taken from Zickel et al. (2016).

range difference between model data of stadial conditions during MIS 3 and the LGM. We calculated the difference in Wm^{-2} per month for each pair of consecutive reference dates, and divided it by 4 to estimate the differences in °C. We then added the difference per month to each day within that month. This of course leads to a slight overestimate of the early days and a slight underestimate of the late days in a month for the first half of the year, and vice versa for the second half. However, given the scope of this study, we consider the differences negligible. In doing so, we can estimate the start, end, length, and summed temperature of the growing season for each insolation reference date.

The following results are shown for single time-slices, as the difference between two consecutive time-slices, and as an accumulated trend over all time-slices. By comparing changes in the spatial distribution of Core Areas between two time-slices, possibly relating to expansions or contractions of human occupation, with changes in insolation, we

TABLE 2. PERCENTAGES OF OVERLAPPING, EXPANDING, AND CONTRACTING CORE AREA SIZES FOR PAIRED PHASES.

Comparison of Two Phases	Map in Figure 9	Sum of Core Areas of Two Phases (km²)	Overlapping Areas %	Expanded Areas %	Contracted Areas %
Aurignacian P1 and P2	(a)	157,750	33	48	18
Aurignacian (all) and *Gravettian P1*	(b)	257,875	34	60	6
Gravettian P1 and *P2*	(c)	272,069	35	11	54
Gravettian P2 and *LGM*	(d)	310,713	28	60	11
LGM and Magdalenian	(e)	494,062	26	38	36

Note that the percentage of overlapping areas is quite constant through time, with decreases towards the Magdalenian due to the overall expansion into northern latitudes.

analysed the impact of these changes on hunter-gatherer populations.

RESULTS ON POPULATIONS SIZES, DISTRIBUTION, AND INSOLATION

PALEODEMOGRAPHIC ESTIMATES

The paleodemographic estimates (see Figure 1) showed an increase in the number of people during the period from 42 to 33 ka (Aurignacian), and to the period between 33 and 29 ka (Early Gravettian). This population growth was followed by a strong decline during the period between 29 and 25 ka (Late Gravettian), with absolute numbers decreasing even below the initial "starting" population at 42 ka. This decline coincided with a withdrawal from the higher latitudes. The period between 25 and 20 ka (Solutrean, Badegoulian, Epigravettian) was a period of population consolidation and renewed growth in Western Europe, while the population in Central Europe remained at low levels. This only changed between 20 and 15 ka, when populations in both Western and Central Europe increased strongly and the higher latitudes were resettled (see Table 1).

In calculating the amount of overlap and discontinuity between the expanding, contracting, newly emerging, and vanishing Core Areas of consecutive time-slices, it was possible to quantify the spatial population dynamics. Here, overlapping Core Areas were seen as indicative of continuity in human presence, whereas expanding or contracting ones were understood as indicating discontinuity. Interestingly, percentages of areas either contracting or expanding varied considerably through time, while spatial overlap of Core Areas for two consecutive phases was constant and covered around 30% (Table 2) of the entire summed area except for the Magdalenian, where the rapid expansion of humans into northern latitudes and the missing data for eastern Central-European sites produced a different pattern, with a reduced percentage of overlap. Generally, the percentage of overlapping Core Areas was surprisingly low, given the constant presence of hunter-gatherers in Western Europe and their quasi-constant presence in Central Europe (see Table 2).

INSOLATION AND GROWING SEASON

An overview of the length, summed temperature, and start of the growing season based on the regional climate model data for LGM and present day is given in Figure 3 and Table 3. The number of days with daily mean temperature above 5°C was obviously much lower for LGM climate conditions, which is in accordance with a much lower summed temperature during the growing season for LGM conditions. Likewise, there was a pronounced shift in the first day of the year when simulated daily mean temperatures rose above 5°C. For present day climate, large parts of Western Europe already reach the first day with mean daily temperature above 5°C in January. For LGM climate conditions, the threshold shifted ~3 months into the year, when mean daily temperatures reached values above 5°C.

When looking at the changes in MJm^{-2} for each month through the succession of the insolation reference dates as differences between consecutive reference dates (Figure 4), it becomes clear that the strongest differences throughout the period of observation occurred during the months from April to October, with differences of up to 60 MJm^{-2} in May and June, while the insolation from December to February remained rather stable.

The accumulated differences throughout the entire period of observation (Figure 5) show that highest losses in solar energy occurred during the months of May and June between 29 and 25 ka, whereas the highest gains can be observed for September and October of the same period.

Figure 6 shows changes in MJm^{-2} throughout the year as differences between two consecutive insolation reference dates. After an initial gain in insolation in the first part of the year and a loss in the second, from 42 to 37.5 ka, each of the following four units (37.5 to 27 ka) showed the opposite trend, with losses in the first half and gains in the second half. From 27 to 25 ka, the loss shifted to the middle of the year, with both the early and late parts of the year gaining energy. From 23.5 ka onwards, the system shifted back to the first pattern, with gains during the first half and losses during the second, but with a much higher amplitude. At 15 ka, a shift of energy gain towards the middle of the year was again observable.

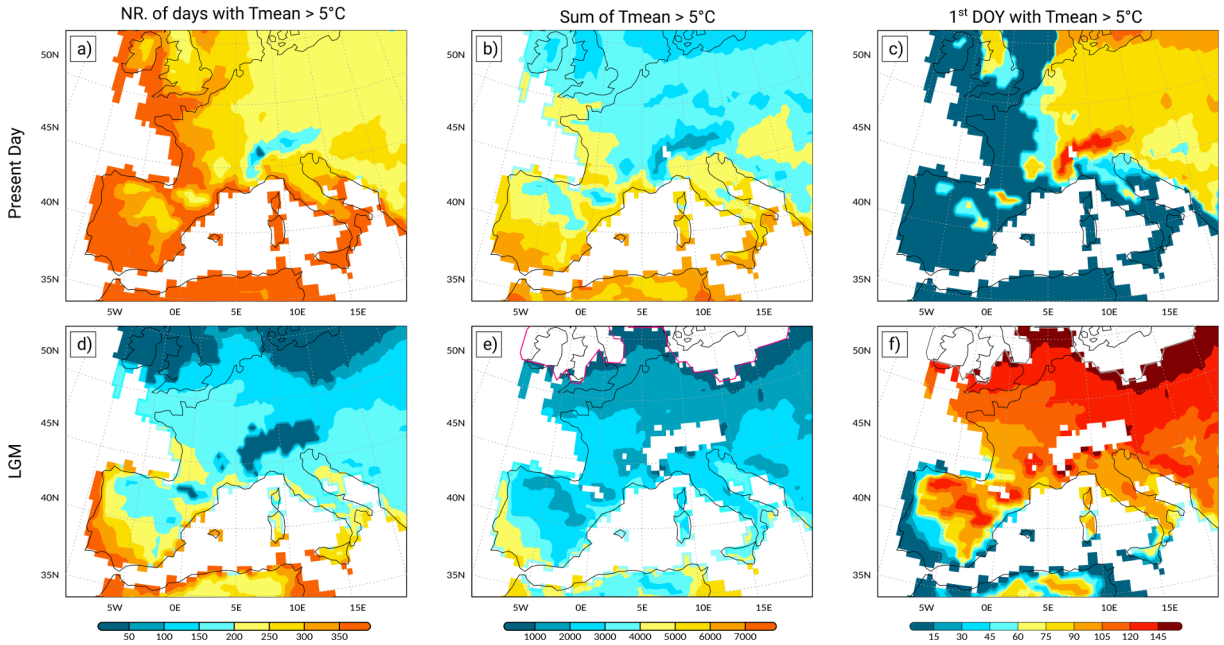

Figure 3. Parameters relevant for the growing season based on WRF model output for present day climate: (a) number of days with a mean daily temperature >5°C; (b) temperature sum of all days within the growing season and (c) the first day of the year with a mean daily temperature >5°C. (d)-(f) same as (a)-(c) but for LGM climate conditions.

Considering the accumulated differences with regard to the position and length of the growing season at 45°N (Figures 7, 8, see Table 3) is very informative, and reveals long-term changes. Three things are particularly remarkable. First, the shift from a gain of insolation during the first half, to a pronounced loss and back to a strong gain with a complementary development during the second half, becomes much clearer. Second, more or less in accordance with this shift, is a delay in the start of the growing season, from mid-April between 42 and 37.5 ka to mid-May between 27 and 25 ka. The end of the growing season also shifted backwards. Third, is the particularly conspicuous loss of solar energy during the start of the growing season between 29 and 21 ka. Between 27 and 25.5 ka, plants had about 60 MJm^{-2} less for their photosynthesis during the crucial early part of the growing season.

TABLE 3. PARAMETERS OF THE GROWING SEASON.

		42 ka	37.5 ka	33 ka	31 ka	29 ka	27 ka	25 ka	23.5 ka	21 ka	20 ka	17 ka	15 ka
50°N	Σ T in°C*	1,772	1,745	1,757	1,753	1,710	1,641	1,557	1,481	1,431	1,464	1,652	1,958
	Start in calender day*	127	125	131	135	141	148	148	148	136	132	123	117
	End in calender day*	261	250	251	259	266	275	279	279	268	264	251	247
	Length in calender days*	135	126	121	125	127	128	132	132	133	134	130	131
45°N	Σ T in°C*	2,572	2,594	2,613	2,546	2,479	2,438	2,018	2,095	2,248	2,282	2,502	2,766
	Start in calender day*	169	166	162	153	152	163	165	168	171	170	170	163
	End in calender day*	107	106	112	122	127	130	132	128	116	113	104	101
	Length in calender days*	275	271	273	274	278	291	295	295	286	282	272	263
	Σ T in C° of first 30 days	291	320	317	341	314	277	267	253	261	279	312	338

*All values represent averages from seven longitudes at -1°, 3.5°, 8°, 12.5°, 17°, 21.5°, and 26° E.

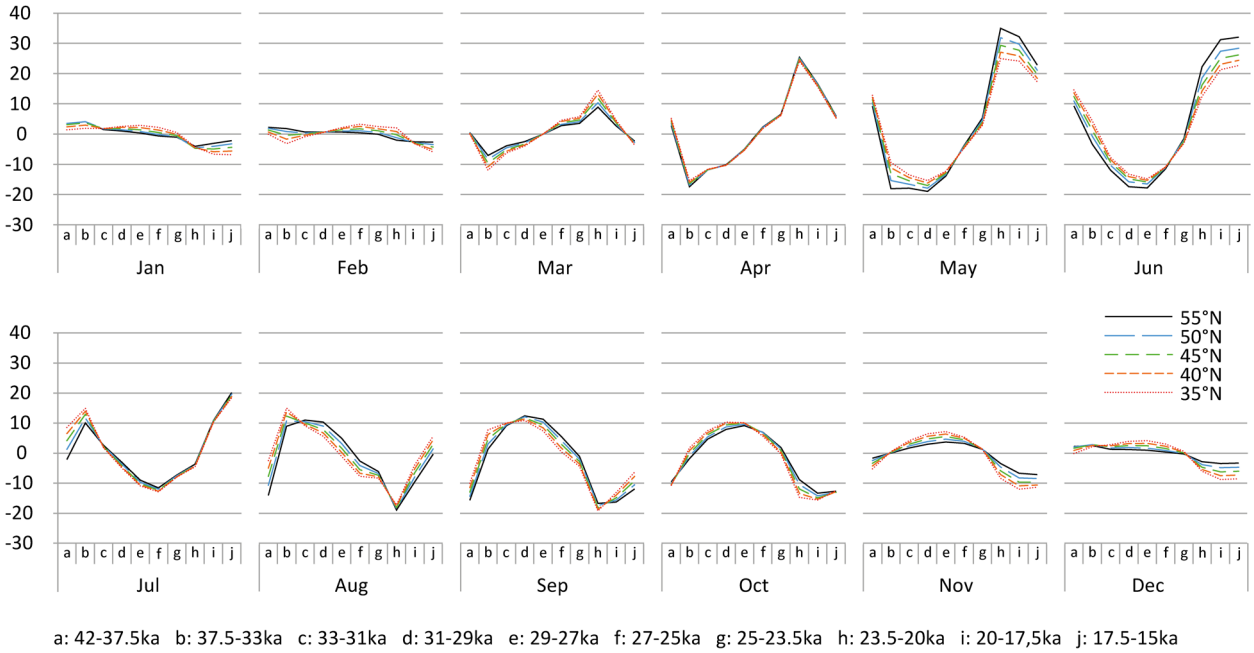

Figure 4. Differences in MJm^{-2} for each month through the succession of the insolation reference dates as differences between two consecutive reference dates.

DISCUSSION

A DIACHRONIC COMPARISON OF POPULATION DYNAMICS AND CHANGES IN SOLAR INSOLATION

In order to assess the possible impact of changes in insolation on the demographic developments of the Upper Paleolithic in Europe, we compared the results of both analyses diachronically. Here, shifts in Core Areas were taken as indicators for spatial population dynamics.

42–33 ka — Aurignacian

For this period connected with the first extensive spread of anatomically modern humans into Central and Western Europe, we estimated a mean population size of 1,500 persons (max. 1,800 / min. 700; Schmidt and Zimmermann

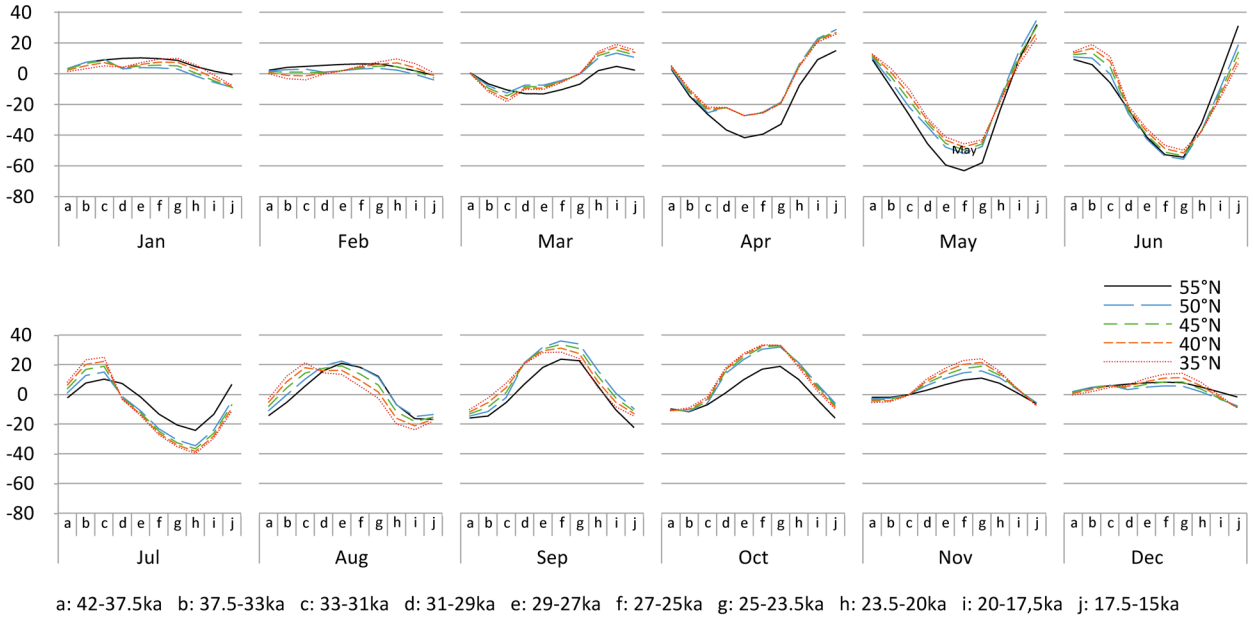

Figure 5. Differences in MJm^{-2} for each month through the succession of the insolation reference dates as accumulated differences throughout all reference dates. For legend, see Figure 4.

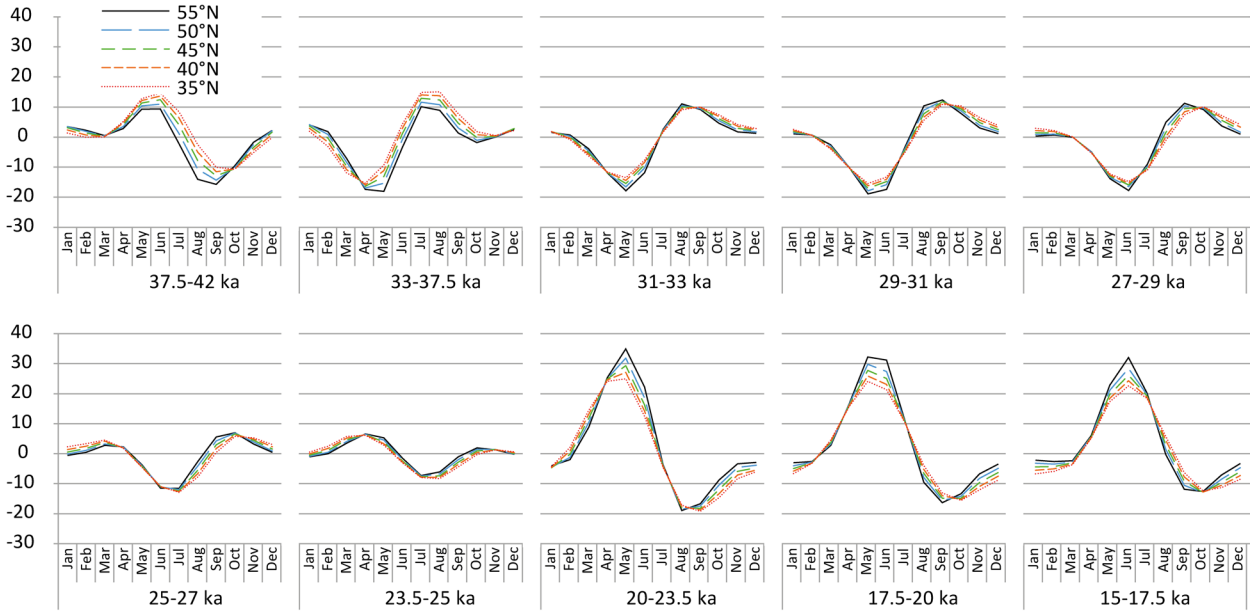

Figure 6. Changes in MJm^{-2} throughout the year as differences between two consecutive insolation reference dates. For legend, see Figure 4.

2019). Core Areas were calculated for an early phase (Proto and Early Aurignacian; Aur P1) and later phases (Aur P2; see Figure 2a, b), although paleodemographic estimates for these two sub-phases were not possible and are therefore given for the entire Aurignacian (Aurignacian all, see Table 1) (Schmidt and Zimmermann 2019). It becomes clear that both phases show regional differences in their spatial pattern and several indicators (e.g., number of sites per 1000 years, size of the Core Areas) support a population increase from the early to the late phase, particularly in the eastern part of the investigated area. Continuity through both phases can be attested for regions where viable populations have been estimated for the entire Aurignacian (Schmidt and Zimmermann 2019: see Figure 2 and Table 4). However, almost 60% of the area covered during the later phase relates to newly emerging and expanding Core Areas (see

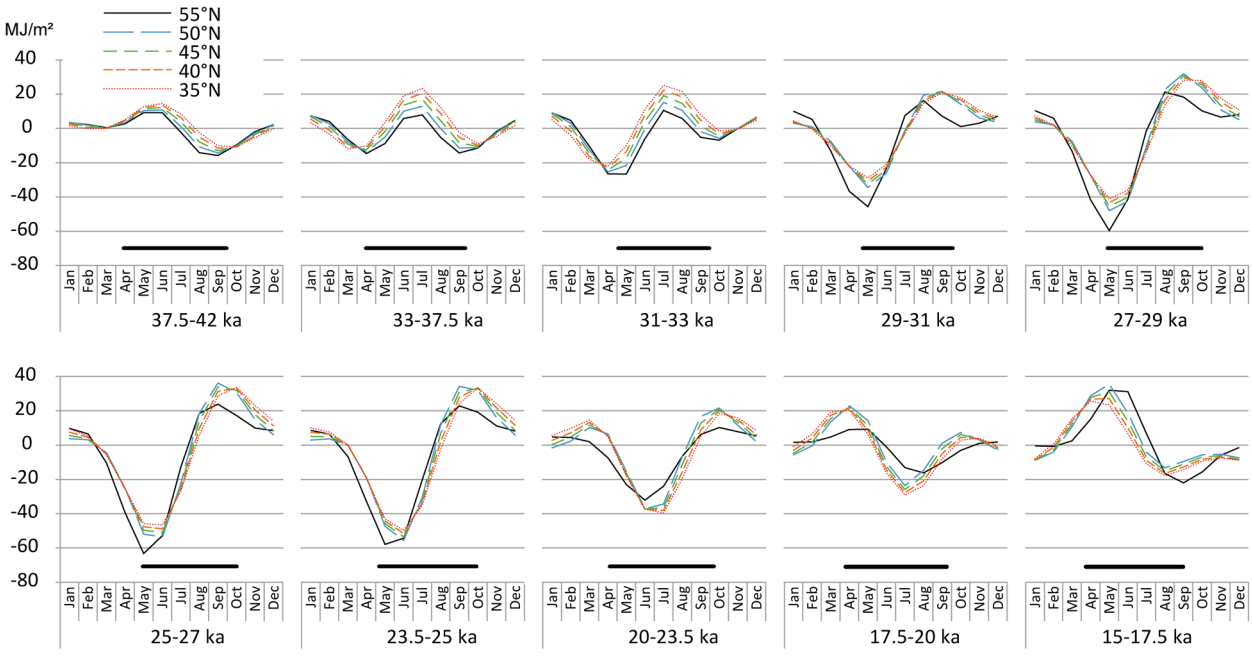

Figure 7. Changes in MJm^{-2} throughout the year as accumulated differences between consecutive insolation reference dates. Solid bars indicate position and length of the growing season at 45°N (see Table 4). For legend, see Figure 4.

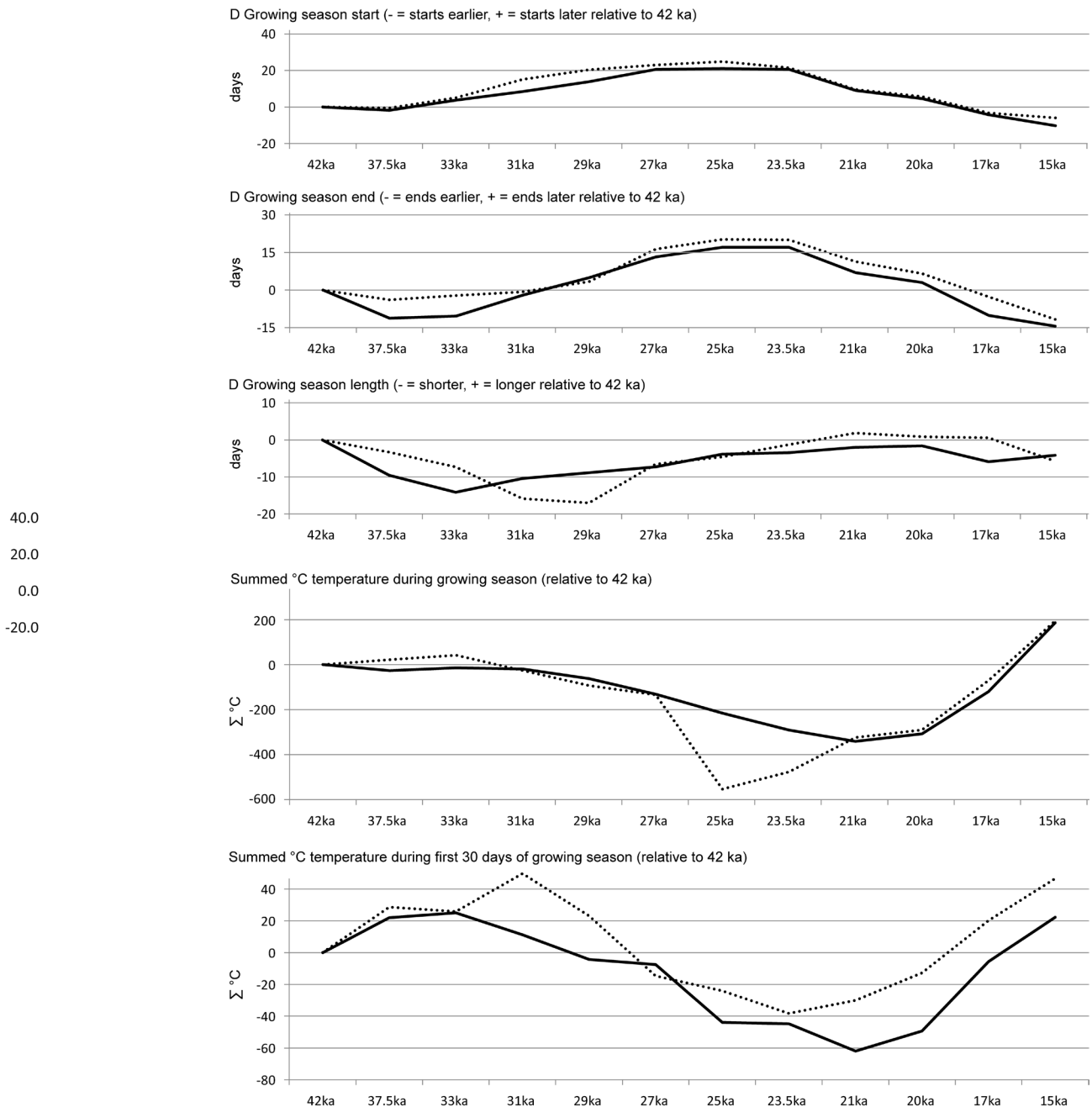

Figure 8. Changes in start, end, length, summed temperatures, and summed temperatures during the first 30 days of the growing season at 45°N (dotted line) and 50°N (solid line).

TABLE 4. QUANTIFICATION OF DIACHRONIC CHANGES IN CORE AREA SIZES.

Phase	Core Areas (km²)	Continuity	Discontinuities		Percentage of Areas Within a Single Phase			
		overlapping areas	expansion in comparison to previous phase	contraction in comparison to subsequent phase	overlapping in comparison to previous phase	expansion in comparison to previous phase	Sum	contraction in comparison to subsequent phase
		(km²)	(km²)	(km²)	%	%	%	%
Aurignacian	103,686	n.a.	n.a.	14,836	n.a.	n.a.	n.a.	14
Aur P1 (Proto/Early)	*81,900*	*n.a.*	*n.a.*	*29,150*	*n.a.*	*n.a.*	*n.a.*	*36*
Aur P2 (Late)	*128,600*	*52,750*	*75,850*	*n.a.*	*41*	*59*	*100*	*n.a.*
Gravettian P1	**243,039**	88,850	154,189	148,259	37	63	*100*	61
Gravettian P2	**123,810**	94,780	29,030	35,300	77	23	*100*	29
Last Glacial Maximum	**275,413**	88,510	186,903	161,113	32	68	*100*	58
Magdalenian	**332,949**	114,300	218,649	n.a.	40	60	*100*	n.a.

Size and percentage of overlapping, contracting, and expanding Core Areas are compared for each phase to previous (areas of overlap and expansion) and subsequent phases (areas of contraction).

Table 4), occurring mainly in Northern Iberia, SW France and the Middle Danube/Moravian Region (Figure 9a).

With regard to the environmental data, we observed some changes. While there is a slight trend towards a later start and shortening of the growing season (see Figure 8), the summed temperature rose during the entire growing season and in the first 30 days, with a first peak of the latter at 37.5 ka and of the former at 33 ka (see Table 3). This gain seems to be more pronounced in Central than in Western Europe. Between 42 and 37.5 ka we see a rise in solar energy during the early growing season, followed by a shift of maximum insolation to the middle part of the year between 37.5 and 33 ka (see Figure 7).

33–29 ka—Early Gravettian

The demographic trend continues during the first half of the Gravettian, and the overall estimate of people rises to a median of 2,800 (+900 / -1,100; Maier and Zimmermann 2017). Core Areas with viable populations during the Aurignacian expanded, especially in the Upper and Middle Danube/Moravian Regions, and new ones emerged across the entire TAC, extending to the East and Southwest of Europe (Figure 9b). Again, the areal increase was around 60%, with an exceptionally low "loss" of regions covered by Core Areas during the Aurignacian (only 14%). Estimated population density within the Core Areas, however, varies considerably, from 2.7 to 0.3 persons per 100km² (median often around 1.4, Maier and Zimmermann 2017).

A look at the environmental data shows that this phase is characterized by a continuation of the moderate decline during the first half of the year, coinciding with a slight delay in the onset of the growing season in comparison to previous periods (see Figures 7 and 8). This trend is counteracted, however, by a strong gain in temperatures during the first 30 days of the growing season, with the highest values of the entire period of observation at 31 ka (see Figure 8).

29–25 ka—Late Gravettian

The most exceptional and marked decrease in population size and distribution during the entire Upper Paleolithic of Europe was detected for the later phase of the Gravettian (Figure 9c), with estimates dropping to a median value of 1,000 (+500 / -300; Maier and Zimmermann 2017). Core Areas disappear in Western Central Europe and experience considerable contraction and fragmentation in all other regions of Europe, except for central Portugal. In comparison with the first half of the Gravettian, the spatial loss amounts to 61% (see Table 4, see also Table 2). Only a few Late Gravettian Core Areas actually show evidence of an expansion (23%), and thus it is not surprising that the Core Areas of the Late Gravettian lie—also to an exceptionally high percentage of 77%—within the areas already occupied previously.

Interestingly, the strong demographic decline coincides with the maximum delay in the start of the growing season coupled with the maximum loss of solar energy during its early phase (see Figure 7). At the same time, the sum of temperatures during the growing season drops sharply towards 25 ka, to the lowest values in the entire period of observation (see Figure 8). The renewed prolongation of the length of the growing season back to the level of 33 ka apparently does not counteract these effects. In this context it is interesting to note the cave bear, a species that was apparently reliant on high-quality plant food, which made it vulnerable to decreasing vegetational productivity, goes extinct in Central Europe at around 28 ka (Pacher and Stuart 2008).

25–20 ka—The Last Glacial Maximum: Solutrean, Badegoulian, Early Epigravettian

During the Last Glacial Maximum, we see a turnaround in the demographic downward trend. Mean population estimates of 3,100 (+3,200 / -1,800) show renewed population growth (Maier et al. 2016). However, it is only in Western Europe that this growth is apparent, whereas populations in Central Europe remained at a low level. Furthermore, increasing the temporal resolution within this period of 5 ka, it seems that there is no evidence of hunter-gatherers north of 47°N between roughly 22 and 21 ka. Previous tendencies towards fragmentation of Core Areas disappear in southwestern / northern Iberia, and turn into expansion

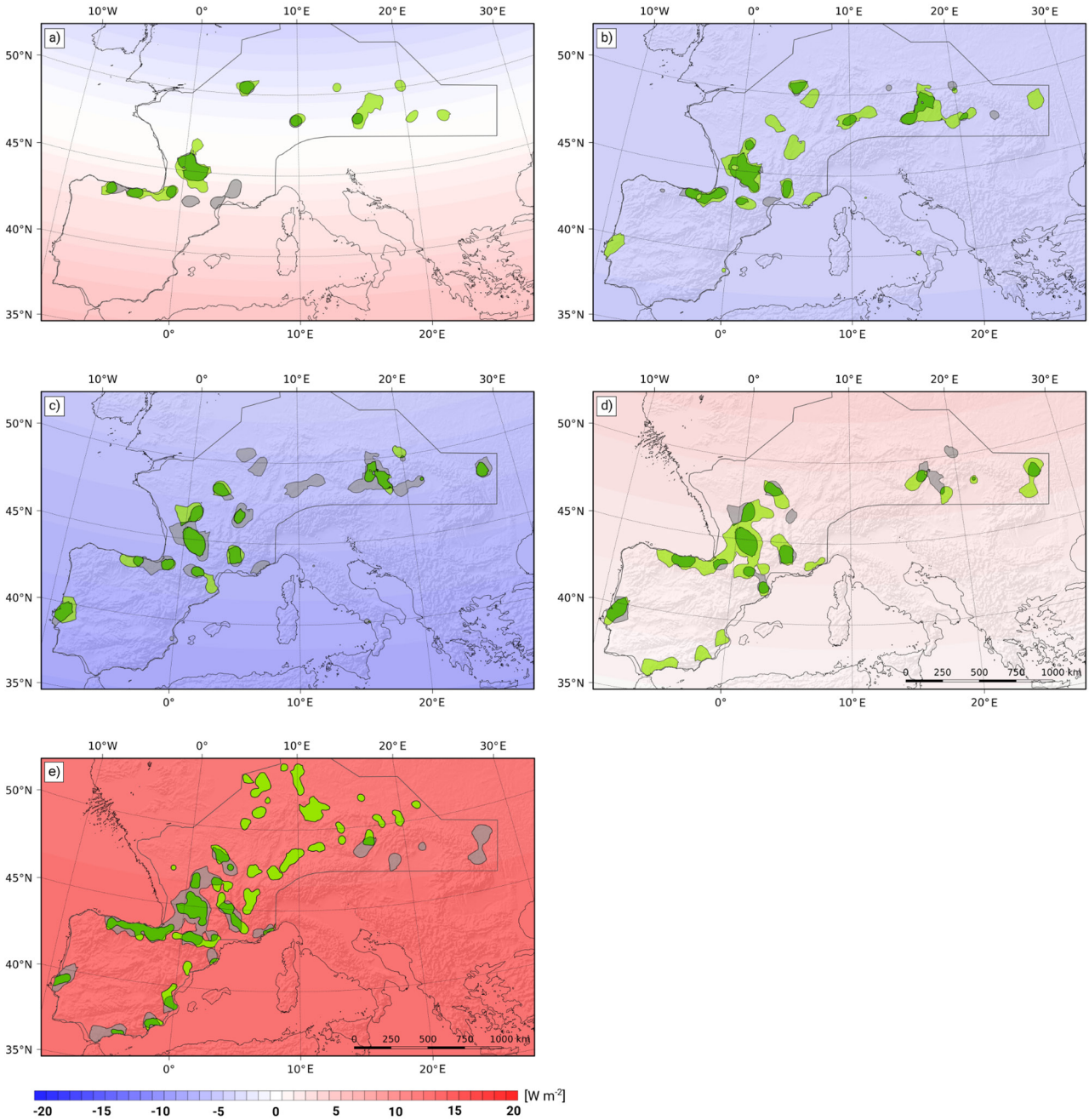

Figure 9: Diachronic changes of Insolation and Core Areas during the Upper Paleolithic. Core Areas are displayed for two successive periods. Colors indicating continuity (dark green), expansion (light green) and contraction (grey areas) of Core Areas. Changes in insolation (W/m², see legend) during the respective phases are given as the difference between insolation at the end of each phase. a) Difference of insolation between 37.5 and 33 ka (Aurignacian P1 and P2); b) between 33 and 29 ka (Aurignacian all and Gravettian P1); c) between 29 and 25 ka (Gravettian P1 and P2); d) between 25 and 20 ka (Gravettian P2 and LGM); e) between 20 and 15 ka (LGM and Magdalenian). For reconstructed coastlines and TAC, see Figure 2.

and even merging of Core Areas (Figure 9d). In southern Iberia, the Cologne Protocol detected Core Areas along the Mediterranean coast for the first time.

Environmentally, we again see an increasingly early start of the growing season, and the growing season length even peaks at 21 ka. After a minimum at 23.5 ka, the summed temperatures of the first 30 days of the growing season rise again, as does the sum of temperature during the entire growing season. In addition, we see a slight increase in solar energy during the first half of the year between 25 and 23.5 ka, becoming a bit more pronounced between 23.5 and 20 ka. However, Verpoorte (2009) noted a marked decline in the diversity of the faunal assemblages of Central Europe occurring at around 24 ka. A similar

pattern was reported by Jochim (1987) for south-western France. This might be related to a delay in the faunal response, because of a certain inertia of population dynamics with regard to change in the environmental system.

20–15 ka—Magdalenian

Between 20 and 15 ka, the estimated number of people rises markedly to a mean of 7,700 (+3,000 / -2,800), while the density in Core Areas ranges between 1.6 and 3.6 persons per 100km² (Kretschmer 2015). With regard to spatial dynamics, it has to be stated that Core Areas are only available for Western Europe and the western part of Central Europe, since Epigravettian sites, located further East, have not been considered in the estimates. This does, to some extent, explain the relatively high percentages (58%) of contracting areas compared to the period of the LGM given in Table 3. Other contractions can be observed in south-western Europe (Figure 9e). However, the general trend of continuity (40%) and expansion (60%) in the spatial distribution of final Magdalenian Core Areas already observed during the LGM does continue—together with the increasing population and the resettlement of the higher latitudes, we see an increasingly early start of the growing season (the earliest of the entire study at 15 ka), coupled with increasing summed temperatures for both the entire growing season (highest in the entire study at 15 ka) and the first 30 days (second highest after 31 ka; see Figure 8). In addition, there is a strong increase in solar energy during the first half of the year, and thus also during the beginning of the growing season (see Figure 7).

INSOLATION AS A PACEMAKER FOR LONG-TERM DEMOGRAPHIC DEVELOPMENTS?

For Paleolithic hunter-gatherers, who extracted all their energy directly from their environment without further manipulation (such as stock keeping or farming), the availability and diversity of animal biomass was probably a key factor allowing their continued presence in a region (Tallavaara et al. 2018). For Western and Central Europe, terrestrial herbivores were the most important game. In addition to their role in human nutrition, they also provided useful raw materials, such as antler, bone, or ivory, making them crucial in the entire subsistence system (Soulier 2014; Soulier et al. 2014). The abundance and diversity of herbivores in a landscape depends essentially on the availability and quality of plant food in a region (Olff et al. 2002).

Usually when thinking about availability of (plant) food, quantity and quality are the factors being considered. However, timing also seems to be of major importance. After long glacial winters, herbivorous animals depend on the availability of sufficient high-quality plant food in spring. Not only do they have to replenish their reserves, but this is also the period when their offspring are born. Spring is thus a crucial period for herbivorous animals and one during which they are rather vulnerable to shifts in plant phenology and environmental stress (Debeffe et al. 2019). The green-up of the landscape is also a key factor for the timing and movements of ungulates for spring migration (Merkle 2016). Shifts, delays, and unforeseen changes in the migration patterns of their most important prey species, in turn, have a high potential to cause problems for hunter-gatherers (Krupnik 2018; Mandryke 1993; Smith 1978). As shown above, spring is the period affected the most by the changes in solar insolation between 43 and 15 ka. Between 25 and 23.5 ka, the growing season was delayed by about a month. Moreover, when it started, the available solar energy and temperatures were very low. Low temperatures also have negative influence on seed germination and seedling establishment (Trugdill et al. 2000; Zhang et al. 2018). The cooling effect of permafrost on soil temperature likely further hampered germination at 25 ka, impeding the start of the growing season, and thus biomass production, even more strongly than estimated from insolation alone. Additionally, a lower CO_2 level (Van Meerbeeck et al. 2009) probably reduced the growth of at least C_3 plants (Bartlein et al. 2010), and waterlogging in the active layer of permafrost soils likely further handicapped plant growth. Impeded germination eventually leads to fewer mature plants and seeds for the following year, leading to a self-reinforcing reduction of the vegetation. It can thus be surmised that between 25 and 23.5 ka, plant food was available only considerably later during the year, and when it appeared, overall biomass production was rather low. This likely caused substantial problems and environmental stress for herbivorous populations, especially in higher latitudes (Belovsky 1988; Mandryk 1993: 56). Such a shift in seasonality, with a prolongation of the winter period and a severely delayed start of the growing season, might also explain the peculiar finding of virtual absence of mammoth during the LGM in large parts of Europe (Stuart 2005). With their high demand for plant food, the carrying capacity during springtime may have been too low to support a viable mammoth population.

The changes in solar insolation and the dependent vegetational system probably led to a loss of animal diversity, delayed spring migrations, and eventually a strong reduction and/or withdrawal of larger herbivores from higher latitudes. In combination, these factors probably made the northern areas also inhospitable for hunter-gatherers, who apparently vanished from these regions. However, the lower latitudes were also affected by decreasing spring insolation, with presumably negative effects on the net production of primary biomass; this is congruent with a general population decline at around 25 ka in Western and Central Europe. It is only with a renewed increase in spring insolation, and an ever-earlier start to the growing season after 20 ka, that populations in Western and Central Europe showed a considerable increase in numbers and densities and an expansion of their Core Areas into the higher latitudes.

Ultimately, it can be stated that this parallel development in paleodemography and solar insolation is unlikely to be merely coincidental. It seems that for the spatially large-scale and long-term development of hunter-gatherer populations, in terms of both their numbers and distribution, solar insolation was an important driver.

CONCLUSION

It seems that ecosystems in Europe between 43 and 15 ka reacted very sensitively to gains and losses in solar energy and the potentially resulting changes in plant and animal phenology. This effect seems to have been particularly pronounced in the higher latitudes (cf. Feurdean et al. 2014), but affected the lower ones as well. Stronger reactions in the north are likely a consequence of generally lower temperatures and insolation values. Hence, while a reduction in the lower latitudes still left enough energy for a timely start of the growing season, a reduction at higher latitudes may have had quite noticeable and rather severe consequences. For hunter-gatherers depending on the resources provided by their environment, it is not the total amount of annual insolation that is important. Rather it is the available energy during the growing season that, via plant biomass and herbivorous animals, affected the basis of existence of Paleolithic hunter-gatherers. Interestingly, a late onset of the growing season seems to have more severe consequences for the ecosystem than a shorter duration.

Anatomically modern humans arrived in Europe during a period of medium intensity solar insolation. Subsequently, a moderate gain in insolation during the growing season was accompanied by moderate population growth and spatial extension of the Core Areas. Over the following millennia, the coupled effects of a late start to the growing season, a reduced amount of energy during its early phase, and a low overall temperature throughout its duration likely led to a considerable reduction in plant biomass availability until around 23.5 ka. It is highly likely that this development led to a reduction of the diversity and abundance of herbivorous animals in the landscape, and might be part of the explanation for the virtual absence of mammoth during the LGM. We hence argue for assuming an indirect causal relationship, mediated by changes in animal abundance, between the decline of solar insolation and the pronounced decline of hunter-gatherer populations in Western and Central Europe between 29 and 25 ka. The same causal relationship can be assumed between the increase in spring insolation, an ever-earlier starting growing season ,and the demographic growth and spatial expansion of hunter-gatherer groups after 23.5 ka ago.

ACKNOWLEDGEMENTS

This publication was funded by the German Research Foundation – Project-ID 57444011 – SFB 806 "Our Way to Europe." We thank the editors and two anonymous reviewers as well as Jayson Orton for his insightful comments on content and the English language, and Nina Avci for assistance during editing. All mistakes are our own.

REFERENCES

Bartlein, P.J., Harrison, S.P., Brewer, S., Connor, S., Davis, B.A.S., Gajewski, K., Guiot, J., Harrison-Prentice, T.I., Henderson, A., Peyron, O., Prentice, I.C., Scholze, M., Seppä, H., Shuman, B., Sugita S., Thompson, M.R.S., Viau, A.E., Williams, J., and Wu, H. 2010. Pollen-based continental climate reconstructions at 6 and 21 ka: a global synthesis. *Climate Dynamics* 37, 775–802. doi:10.1007/s00382-010-0904-1.

Berger, A.L. 1978. Long-term variations of daily insolation and Quaternary climatic changes. *Journal of the Atmospheric Sciences* 35, 2362–2367.

Bocquet-Appel, J.-P. and Demars P.-Y. 2000. Population kinetics in the Upper Palaeolithic in Western Europe. *Journal of Archaeological Science* 27, 551–570.

Bocquet-Appel, J.-P., Demars, P., Noiret, L., and Dobrowsky, D. 2005. Estimates of Upper Palaeolithic meta-population size in Europe from archaeological data. *Journal of Archaeological Science* 32, 1656–1668.

Boserup, E. 1965. T*he Conditions of Agricultural Growth. The Economics of Agrarian Change Under Population Pressure*. UK: Allen & Unwin Ltd, London.

Both, C., Van Turnhout, C.A.M., Bijlsma, R.G., Siepel, H., Van Strien A.J., and Foppen, R.P.B. 2010. Avian population consequences of climate change are most severe for long-distance migrants in seasonal habitats. *Proceedings of the Royal Society B* 277, 1259–1266. doi:10.1098/rspb.2009.1525.

Bradtmöller, M., Pastoors, A., and Weniger, G.-C. 2010. The repeated replacement model - Rapid climate change and population dynamics in Late Pleistocene Europe. *Quaternary International* 247, 38–49. doi: 10.1016/j.quaint.2010.10.015.

Braconnot, P., Harrison, S.P., Kageyama, M., Bartlein, P.J., Masson-Delmotte, V., Abe-Ouchi, A., Otto-Bliesner, B., and Zhao, Y. 2012. Evaluation of climate models using paleoclimatic data. *Nature Climate Change* 2, 417–424. doi:10.1038/nclimate1456.

Burrows, M.T., Schoeman, D.S., Buckley, L.B., Moore, P., Poloczanska, E.S., Brander, K.M., Brown, C., Bruno, J.F., Duarte, C.M., Halpern, B.S., Holding, J., Kappel, C.V., Kiessling, W., O'Connor, M.I., Pandolfi, J.M., Parmesan, C., Schwing, F.B., Sydeman, W.J., and Richardson, A.J. 2011. The pace of shifting climate in marine and terrestrial ecosystems. *Science* 334, 652–655. doi:10.1126/science.1210288.

Crucifix, M. 2016. palinsol: Insolation for Palaeoclimate Studies. R package version 0.93. https://CRAN.R-project.org/package=palinsol.

Debeffe, L., Rivrud, I. M., Meisingset, E. L., and Mysterud, A. 2019. Sex-specific differences in spring and autumn migration in a northern large herbivore. *Scientific Reports* 9, 6137. https://doi.org/10.1038/s41598-019-42639-3.

Demidenko, Y. 2018. Gravettian in the Great North Black Sea Region in the context of East European Upper Palaeolithic. *Stratum Plus* 1, 265–283.

Feurdean, A., Perşoiu, A., Tanţău, I., Stevens, T., Magyari, E.K., Onac, B.P., Marković, S., Andrič, M., Connor, S., Fărcaş, S., Gałka, M., Gaudeny, T., Hoek, W., Kolaczek, P., Kuneš, P., Lamentowicz, M., Marinova, E., Michczyńska, D., Perşoiu, I., Płóciennik, M., Słowiński, M., Stancikaite, M., Sumegi, P., Svensson, A., Tămaş, T., Timar, A., Tonkov, S., Toth, M., Veski, S., Willis, K.J., and Zernitskaya, V. 2014. Climate variability and as-

sociated vegetation response throughout Central and Eastern Europe (CEE) between 8 and 60 kyrs ago. *Quaternary Science Reviews* 106, 206–224.

French, J.C. 2015. Demography and the Palaeolithic archaeological record. *Journal of Archaeological Method and Theory* 23, 150–199.

French, J.C. 2018. Archaeological demography as a tool for the study of women and gender in the past. *Cambridge Archaeological Journal* 29, 1–17.

French, J.C. and Collins, C. 2015. Upper Palaeolithic population histories of Southwestern France: a comparison of the demographic signatures of 14C date distributions and archaeological site counts. *Journal of Archaeological Science* 55, 122–134.

Fu, Q., Posth, C., Hajdinjak, M., Petr, M., Mallick, S., Fernandes, D., Furtwängler, A., Haak, W., Meyer, M., Mittnik, A., Nickel, B., Peltzer, A., Rohland, N., Slon, V., Talamo, S., Lazaridis, I., Lipson, M., Mathieson, I., Schiffels, S., Skoglund, P., Derevianko, A.P., Drozdov, N., Slavinsky, V., Tsybankov, A., Grifoni Cremonesi, R., Mallegni, F., Gély, B., Vacca, E., González Morales, M.R., Straus, L.G., Neugebauer-Maresch, C., Teschler-Nicola, M., Constantin, S., Moldovan, O. T., Benazzi, S., Peresani, M., Coppola, D., Lari, M., Ricci, S., Ronchitelli, A., Valentin, F., Thevenet, C., Wehrberger, K., Grigorescu, D., Rougier, H., Crevecoeur, I., Flas, D., Semal, P., Mannino, M.A., Cupillard, C., Bocherens, H., Conard, N.J., Harvati, K., Moiseyev, V., Drucker, D.G., Svoboda, J., Richards, M.P., Caramelli, D., Pinhasi, R., Kelso, J., Patterson, N., Krause, J., Pääbo, S. and Reich, D. 2016. The genetic history of Ice Age Europe. *Nature* 534, 200–205.

Gamble, C.S. 1999. *The Palaeolithic Settlement of Europe*. Cambridge University Press, Cambridge.

Gamble, C., Davies, W., Pettitt, P., and Richards, M. 2004. Climate change and evolving human diversity in Europe during the Last Glacial. *Philosophical Transactions of The Royal Society B* 359, 243–254. doi:10.1098/rstb.2003.1396.

Gienapp, P., Reed, T.E., and Visser, M.E. 2014. Why climate change will invariably alter selection pressures on phenology. *Proceedings of the Royal Society B* 281, 20141611. https://dx.doi.org/10.1098/rspb.2014.1611.

Giorgetta, M.A., Jungclaus, J., Reick, C.H., Legutke, S., Bader, J., Böttinger, M., Brovkin, V., Crueger, T., Esch, M., Fieg,K., Glushak, K., Gayler, V., Haak, H., Heinz-Hollweg, D., Ilyina, T., Kinne, S., Kornblueh, L., Matei, D., Mauritsen, T., Mikolajewicz, U., Mueller, W., Notz, D., Pithan, F., Raddatz, T., Rast, S., Redler, R., Roeckner, E., Schmidt, H., Schnur, R., Segschneider, J., Six, K.D., Stockhause, M., Timmreck, C., Wegner, J., Widmann, H., Wieners, K.-H., Claussen, M., Marotzke, J. and Stevens, B. 2013. Climate and carbon cycle changes from 1850 to 2100 in MPI-ESM simulations for the Coupled Model Intercomparison Project phase 5. *Journal of Advances in Modeling Earth Systems* 5, 572-597. doi:10.1002/jame.20038.

Gosse, G., Varlet-Grancher, C., Bonhomme, R., Chartier, M., Allirand, J.-M., and Lemaire, G. 1986. Production maximale de matière sèche et rayonnement solaire intercepté par un couvert végétal. *Agronomie* 6, 47–56.

Hassan, G.E., Youssef, M.E., Mohamed, Z.E., Ali, M.A., and Hanafy, A.A. 2016. New temperature-based models for predicting global solar radiation. *Applied Energy* 179, 437–450.

Henderson, K. and Loreau, M. 2019. An ecological theory of changing human population dynamics. *People and Nature* 1, 31–43. https://doi.org/10.1002/pan3.8.

Huang, W., Ge, Q., Wang, H., and Dai, J. 2019. Effects of multiple climate change factors on the spring phenology of herbaceous plants in Inner Mongolia, China: evidence from ground observation and controlled experiments. *International Journal of Climatology* 39, 5140–5153. doi:10.1002/joc.6131

Jiang, D., Sui, Y., Lang, X., and Tian, Z. 2018. Last glacial maximum and mid-Holocene thermal growing season simulations. *Journal of Geophysical Research: Atmospheres* 123, 11,466–11,478. https://doi.org/10.1029/2018JD028605.

Jochim, M. 1987. Late Pleistocene refugia in Europe. In T*he Pleistocene Old World: Regional Perspectives*, Soffer, O. (ed.). Plenum Press, New York, pp. 317–331.

Kaplan, J.O., Pfeiffer, M., Kolen, J.C.A., and Davis, B.A.S. 2016. Large scale anthropogenic reduction of forest cover in Last Glacial Maximum Europe. *PLoS One* 11(11): e0166726. doi:10.1371/journal.pone.0166726

Klein, K., Wegener, C., Schmidt, I., Rostami, M., Ludwig, P., Ulbrich, S., Weniger, G.-C., and Shao, Y. 2021. Human existence potential in Europe during the Last Glacial Maximum. *Quaternary International* 581–582, 7–27.

Koch, P.L. and Barnosky, A.D. 2006. Late Quaternary extinctions: state of the debate. *Annual Review of Ecology, Evolution, and Systematics* 37, 215–50. doi:10.1146/annurev.ecolsys.34.011802.132415.

Kretschmer, I. 2015. *Demographische Untersuchungen zu Bevölkerungsdichten, Mobilität und Landnutzungsmustern im späten Jungpaläolithikum*. Verlag Marie Leidorf GmbH, Rahden/Westf.

Krupnik, I. 2018. 'Arctic crashes:' revisiting the human-animal disequilibrium model in a time of rapid change. *Human Ecology* 46, 685–700. https://doi.org/10.1007/s10745-018-9990-1

Ludwig, P., Pinto, J. G., Raible, C.C., and Shao Y. 2017. Impacts of surface boundary conditions on regional climate model simulations of European climate during the Last Glacial Maximum. *Geophysical Research Letters* 44, 5086–5095. doi:10.1002/2017GL073622.

Liu, Q., Fu, Y. H., Zeng, Z., Huang, M., Li, X., and Piao, S. 2016. Temperature, precipitation, and insolation effects on autumn vegetation phenology in temperate China. *Global Change Biology* 22, 644–655. https://doi.org/10.1111/gcb.13081

Maier, A. and Zimmermann, A. 2017. Populations headed south? The Gravettian from a palaeodemographic point of view. *Antiquity* 91, 573–588.

Maier, A., Lehmkuhl, F., Ludwig, P., Melles, M., Schmidt, I., Shao, Y., Zeeden, C., and Zimmermann, A. 2016.

Demographic estimates of hunter-gatherers during the Last Glacial Maximum in Europe against the background of palaeoenvironmental data. *Quaternary International* 425, 49–61.

Mandryk, C.A.S. 1993. Hunter-gatherer social costs and the nonviability of submarginal environments. J*ournal of Anthropological Research* 49, 39–71.

MARGO Project Members. 2009. Constraints on the magnitude and patterns of ocean cooling at the Last Glacial Maximum. *Nature Geoscience* 2, 127–132. doi:10.1038/ngeo411.

Mayor, S.J., Guralnick, R.P., Tingley, M.W., Otegui, J., Withey, J.C., Elmendorf, S.C., Andrew, M.E., Leyk, S., Pearse, I.S., and Schneider, D.C. 2017. Increasing phenological asynchrony between spring green-up and arrival of migratory birds. *Scientific Reports* 7, 1902. doi:10.1038/s41598-017-02045-z.

Merkle, J.A., Monteith, K.L., Aikens, E.O., Hayes, M.M., Hersey, K.R., Middleton, A.D., Oates, B.A., Sawyer, H., Scurlock, B.M., and Kauffman, M.J. 2016. Large herbivores surf waves of green-up during spring. *Proceedings of the Royal Society B* 283, 20160456. https://doi.org/10.1098/rspb.2016.0456.

Monteith, J.L. 1994. Validity of the correlation between intercepted radiation and biomass. *Agricultural and Forest Meteorology* 68, 213–220.

Ohlberger, J., Thackeray, S.J., Winfield, I.J., Maberly, S.C., and Vøllestad, L.A. 2014. When phenology matters: age–size truncation alters population response to trophic mismatch. *Proceedings of the Royal Society B* 281, 20140938. https://dx.doi.org/10.1098/rspb.2014.0938.

Olff, H., Ritchie, M.E., and Prins, H.H.T. 2002. Global environmental controls of diversity in large herbivores. *Nature* 415, 901–904. doi:10.1038/415901a.

Pacher, M. and Stuart, A.J. 2008. Extinction chronology and palaeobiology of the cave bear (*Ursus spelaeus*). *Boreas* 38, 189–206.

Parmesan, C. and Hanley, M.E. 2015. Plants and climate change: complexities and surprises. *Annals of Botany* 116 (6), 849–864. doi:10.1093/aob/mcv169.

Posth, C., Renaud, G., Mittnik, A., Drucker, D.G., Rougier, H., Cupillard, C., Valentin, F., Thevenet, C., Furtwängler, A., Wißing, C., Francken, M., Malina, M., Bolus, M., Lari, M., Gigli, E., Capecchi, G., Crevecoeur, I., Beauval, C., Flas, D., Germonpré, M., van der Plicht, J., Cottiaux, R., Gély, B., Ronchitelli, A., Wehrberger, K., Grigorescu, D., Svoboda, J., Semal, P., Caramelli, D., Bocherens, H., Harvati, K., Conard, N.J., Haak, W., Powell, A. and Krause, J. 2016. Pleistocene mitochondrial genomes suggest a single major dispersal of non-Africans and a Late Glacial population turnover in Europe. *Current Biology* 26, 827–833.

Roebroeks, W. 2006. The human colonization of Europe: where are we? *Journal of Quaternary Science* 21, 425–435.

Sandom, C., Faurby, S., Sandel, B., and Svenning, J.-C. 2014. Global late Quaternary megafauna extinctions linked to humans, not climate change. *Proceedings of the Royal Society B* 281, 20133254. https://dx.doi.org/10.1098/rspb.2013.3254

Schmidt, I. and Zimmermann, A. 2019. Population dynamics and socio-spatial organization of the Aurignacian: scalable quantitative demographic data for western and central Europe. *PLoS One* 14(2), e0211562. https://doi.org/10.1371/journal.pone.0211562

Schmidt, I., Hilpert, J., Kretschmer, I., Peters, R., Broich, M., Schiesberg, S., Vogels, O., Wendt, K.P., Zimmermann, A., and Maier, A. 2021. Approaching prehistoric demography: proxies, scales and scope of the Cologne Protocol in European contexts. Proceedings of the Royal Society B 376, http://dx.doi.org/10.1098/rstb.2019.0714.

Skamarock, W.C., Klemp, J.B., Dudhia, J., Gill, D.O., Barker, D.M., Duda, M.G., Huang, X.-Y., Wang, W., and Powers, J.G. 2008. A description of the advanced research WRF version 3, NCAR Tech. Note NCAR/TN-475+STR. https://doi:10.5065/D68S4MVH.

Smith, J.G.E. 1978. Economic uncertainty in an "original affluent society": caribou and caribou eater Chipewyan adaptive strategies. *Arctic Anthropology* 15, 68–88.

Soulier, M.-C. 2014. L'exploitation alimentaire et technique du gibier au début du Paléolithique supérieur aux Abeilles (Haute-Garonne, France). *Paléo* 25, 287–307.

Soulier, M.-C., Goutas N., Normand, C., Legarnd, A., and White R. 2014. Regards croisés de l'archéozoologue et du technologue sur l'exploitation des ressources animales à l'Aurignacien archaïque: l'exemple d'Isturitz (Pyrénées-Atlantiques, France). In T*ransitions, ruptures et continuité en Préhistoire.* Volume 2: *Exploitation des ressources organiques à la fin du Paléolithique moyen et au début du Paléolithique supérieur: interactions entre environnement et comportements techniques*, Thiébault, C., Claud, É., and Costamagno, S. (eds.). XXVIIe congrès préhistorique de France, Bordeaux-Les Eyzies, 31 mai-5 juin 2010: Mémoires de la SPF, pp 315–332.

Stuart, A.J. 2005. The extinction of woolly mammoth (*Mammuthus primigenius*) and straight-tusked elephant (*Palaeoloxodon antiquus*) in Europe. *Quaternary International* 126–128, 171–177.

Tallavaara, M., Luoto, M., Korhonen, N., Järvinen, H., and Seppä, H. 2015. Human population dynamics in Europe over the Last Glacial Maximum. *Proceedings of the National Academy of Sciences USA* 112, 8232–8237.

Tallavaara, M., Eronen, J.T., and Luoto, M. 2018. Productivity, biodiversity, and pathogens influence the global hunter-gatherer population density *Proceedings of the National Academy of Sciences USA* 115(6), 1232–1237. https://doi.org/10.1073/pnas.1715638115

Trugdill, D.L., Squire, G.R., and Thompson, K. 2000. A thermal time basis for comparing the germination requirements of some British herbaceous plants. *New Phytology* 145, 107–114.

Van Meerbeeck, C.J., Renssen, H., and Roche, D.M. 2009. How did Marine Isotope Stage 3 and Last Glacial Maximum climates differ? – Perspectives from equilibrium simulations. *Climate of the Past* 5, 33–51.

Verpoorte, A. 2009. Limiting factors on early modern human dispersals: the human biogeography of late Pleni-

glacial Europe. *Quaternary International* 201, 77–85.

Weninger, B. and Jöris, O. 2008. A ^{14}C age calibration curve for the last 60 ka: the Greenland-Hulu U/Th timescale and its impact on understanding the Middle to Upper Paleolithic transition in Western Eurasia. *Journal of Human Evolution* 55, 772–781.

Zhang, H., Tian, Y., and Zhou, D. 2018. A modified thermal time model quantifying germination response to temperature for C_3 and C_4 species in temperate grassland. *Agriculture* 5, 412–426. doi:10.3390/agriculture5030412.

Zickel, M., Becker, D., Verheul, J., Yener, Y., and Willmes, C. 2016. Paleocoastlines GIS dataset (CRC806-Database). https://crc806db.uni-koeln.de/maps/ (accessed 02.06.2019).

Zimmermann, A., Hilpert, J., and Wendt, K.P. 2009. Estimations of population density for selected periods between the Neolithic and AD 1800. *Human Biology* 81, 357–380.